JB
Journals.ASM.org

LcrV Mutants That Abolish *Yersinia* Type III Injectisome Function

Katherine Given Ligtenberg,[a,b] Nathan C. Miller,[a,b] Anthony Mitchell,[a,b] Gregory V. Plano,[c] Olaf Schneewind[a,b]

Howard Taylor Ricketts Laboratory, Argonne National Laboratory, Argonne, Illinois, USA[a]; Department of Microbiology, University of Chicago, Chicago, Illinois, USA[b]; Department of Microbiology and Immunology, University of Miami Miller School of Medicine, Miami, Florida, USA[c]

LcrV, the type III needle cap protein of pathogenic *Yersinia*, has been proposed to function as a tether between YscF, the needle protein, and YopB-YopD to constitute the injectisome, a conduit for the translocation of effector proteins into host cells. Further, insertion of LcrV-capped needles from a calcium-rich environment into host cells may trigger the low-calcium signal for effector translocation. Here, we used a genetic approach to test the hypothesis that the needle cap responds to the low-calcium signal by promoting injectisome assembly. Growth restriction of *Yersinia pestis* in the absence of calcium (low-calcium response [LCR$^+$] phenotype) was exploited to isolate dominant negative *lcrV* alleles with missense mutations in its amber stop codon (*lcrV*$_{*327}$). The addition of at least four amino acids or the eight-residue Strep tag to the C terminus was sufficient to generate an LCR$^-$ phenotype, with variant LcrV capping type III needles that cannot assemble the YopD injectisome component. The C-terminal Strep tag appears buried within the cap structure, blocking effector transport even in *Y. pestis yscF* variants that are otherwise calcium blind, a constitutive type III secretion phenotype. Thus, LcrV$_{*327}$ mutants arrest the needle cap in a state in which it cannot respond to the low-calcium signal with either injectisome assembly or the activation of type III secretion. Insertion of the Strep tag at other positions of LcrV produced variants with wild-type LCR$^+$, LCR$^-$, or dominant negative LCR$^-$ phenotypes, thereby allowing us to identify discrete sites within LcrV as essential for its attributes as a secretion substrate, needle cap, and injectisome assembly factor.

Three pathogenic *Yersinia* species—*Yersinia enterocolitica*, *Yersinia pseudotuberculosis*, and *Yersinia pestis*—employ a virulence plasmid-encoded type III secretion machine to establish disease (1–3). The key function of type III secretion machines during the pathogenesis of *Yersinia* infections is the transport of effectors [YopE, YopH, YopM, YopO, YopP (J), YopT, and YopQ] into host cells, thereby enabling bacterial escape from innate immune responses (4, 5). Assembly of the *Yersinia* type III secretion machine involves 23 different protein components encoded by *ysc* genes (Yop secretion), which catalyze the successive secretions of early, middle, and late (effector) substrates (6, 7). During the initial assembly stage of the *Yersinia* type III machine, a protein transport channel with a central conduit is formed across the bacterial inner and outer membranes (8). The type III machine promotes self-assembly of its basal membrane components and secretion of its inner rod (YscI) and needle (YscF) extensions (9, 10), followed by the transport of middle substrates to cap the needle (LcrV, YopD) (11). Contact of capped needles with host cells is thought to promote the assembly of the injectisome in host cell membranes (YopB, YopD) (12, 13). Establishment of a *Yersinia* type III conduit into host cells is associated with a decrease in calcium ions: the concentration of calcium ions is 1.2 mM in extracellular fluids and $<$10 μM within cells (14). Reception of this signal activates the *Yersinia* type III pathway for the translocation of effectors into host cells (14, 15).

Electron microscopy experiments with *Y. enterocolitica* needle complexes revealed the LcrV cap (11). Like *Y. pestis yscF* mutants, *lcrV* variants are unable to complete the type III conduit into host cells and cannot activate the pathway even when calcium ions are chelated (3, 16, 17). A different phenotype has been observed for *yopB* and *yopD*; *Yersinia* mutants lacking *yopB* or *yopD* respond to the low-calcium signal with type III secretion, yet these variants are unable to direct effectors into host cells (18, 19). When extracellular calcium ions are removed, wild-type *Y. pestis* cannot form colonies on laboratory media at 37°C (low-calcium response [LCR$^+$] phenotype) (20); however, this growth restriction is abolished when *yscF* or *lcrV* is deleted (LCR$^-$) (3, 21). In contrast, *Y. pestis* calcium-blind mutants secrete effectors even in the presence of extracellular calcium ions and cannot form colonies at 37°C (temperature sensitive for growth [*ts*] phenotype) (22). Torruellas and colleagues isolated *yscF* variants with calcium-blind *ts* phenotypes (21). These YscF mutants harbor single amino acid substitutions of negatively charged aspartic acid residues with neutral amino acids, suggesting that the association of aspartyl with calcium ions may enable the needle protein to act as a calcium sensor (21). The LCR pathway also involves factors in the *Y. pestis* cytoplasm. For example, LcrG and LcrE (YopN) are required for the *Y. pestis* blockade of effector secretion in the presence of calcium, as *lcrG* and *lcrE* mutants also display calcium-blind *ts* phenotypes (22–24). LcrG binds LcrV in the bacterial cytoplasm, and this association is required for LcrV secretion (17, 25).

LcrV, but not any other component of the type III pathway, is the plague-protective antigen; antibodies that bind LcrV prevent *Y. pestis* translocation of effectors into host cells (26, 27). Although wild-type LcrV could not be crystallized, the structure of a variant (K40A/D41A/K42A) was revealed by X-ray crystallography (28). Of note, the N and C termini of LcrV (residues 23 to 27 and 323 to 326), Y^{90}, and

Received 21 October 2012 **Accepted** 29 November 2012
Published ahead of print 7 December 2012
Address correspondence to Olaf Schneewind, oschnee@bsd.uchicago.edu.
K.G.L., N.C.M., and A.M. contributed equally to this article.
Supplemental material for this article may be found at http://dx.doi.org/10.1128/JB.02021-12.

doi:10.1128/JB.02021-12

two internal loops (residues 49 to 63 and 260 to 275) were not visible in the electron density map (28). $LcrV_{K40A/D41A/K42A}$ assumed an overall dumbbell-shaped structure with a central coiled coil connecting two globular folds (28). This structure was modeled into high-resolution electron microscopy images of the LcrV needle cap, which suggest an atomic model for a pentameric LcrV ring (13). The functional relevance of the proposed structure is, however, not clear. The LcrV residues involved in forming a central conduit, in associating with the needle protein (YscF), or in forming the injectisome (YopB and YopD) are not yet known. Furthermore, although the aforementioned hypothesis proposes a dynamic role for LcrV in capping type III needles and in promoting injectisome assembly, experimental proof for this conjecture is still missing. Here, we used genetic as well as molecular biology approaches to address these questions.

MATERIALS AND METHODS

Bacterial strains and plasmids. *Y. pestis* strain KIM D27 (wild type) (29) and the Δ*lcrV* mutant (KLD29) (27) were grown in heart infusion broth (HIB), M9-Casamino Acids (M9-Ca) minimal medium, or thoroughly modified Higuchi's (TMH) medium (27, 29, 30). *Y. enterocolitica* strain W22703 (wild type) (31) and the Δ*lcrV* mutant (CT1) (17) were grown in tryptic soy broth (TSB) or M9-Ca medium, as indicated. Chloramphenicol was added to *Y. enterocolitica* (30 μg/ml) or *Y. pestis* (10 μg/ml) cultures for plasmid retention. For PCR mutagenesis experiments, determination of the low-calcium response (LCR) was performed on solid medium by plating *Y. pestis* cultures onto tryptose blood agar (TBA) plates containing 20 mM $MgCl_2$, 20 mM sodium oxalate, and 1 mM isopropyl-β-D-thiogalactopyranoside (IPTG). Duplicate plates were inoculated with transformants and incubated at 26°C or 37°C for 48 h and then scored for their LCR.

The construction of the p$lcrV_{W22703}$ (pNM142) and p$lcrV_{D27}$ (pNM77) mutants has been described previously (33). PCR mutagenesis of the p$lcrV_{D27}$ mutant (harboring *Y. pestis* KIM D27 *lcrV*) was performed with the GeneMorph II EZClone domain mutagenesis kit (Agilent) using primers complementary to the vector backbone at positions approximately 60 bp outside the *lcrV* coding region: 5′-TGCGCCGACATCATA ACGGTTC-3′ (pHSG lcrV 5′) and 5′-TCTGCCTCCCAGAGCCTGAT A-3′ (pHSG lcrV 3′). Plasmids carrying the LcrV-Strep alleles of *Y. enterocolitica* were generated with the QuikChange Lightning site-directed mutagenesis kit (Agilent) with reverse complementary primers containing the Strep tag sequence (5′-TGGTCTCATCCTCAATTTGAG AAG-3′), and plasmids harboring the sequential C-terminal additions of the Strep tag amino acid residues to $LcrV_{D27}$ (p$lcrV_{+1}$, p$lcrV_{+2}$, p$lcrV_{+3}$, p$lcrV_{+4}$, p$lcrV_{+5}$, p$lcrV_{+6}$, p$lcrV_{+7}$) were assembled in a similar manner. Standard methods for transformation of the plasmids into *Y. pestis* were employed.

LCR growth assay. To determine the bacterial growth phenotypes in the presence and absence of calcium, overnight cultures of *Y. pestis* were diluted 1:40 into 4 ml of TMH medium and incubated for 2 h at 26°C, at which time 200-μl aliquots of each sample were added in triplicate to a sterile 96-well flat-bottom growth plate (wells were supplemented in advance, where necessary, by the addition of $CaCl_2$ and IPTG to final concentrations of 2.5 mM and 1 mM, respectively). Bacterial growth at 37°C was recorded by a plate reader over a period of 12 h by measuring the optical density at 600 nm for shaking cultures containing TMH medium alone or TMH medium supplemented with 2.5 mM $CaCl^{2+}$.

***Yersinia* type III secretion.** To monitor secretion into the extracellular environment, *Y. pestis* and *Y. enterocolitica* overnight cultures were diluted 40-fold into 4 ml M9-Ca medium or TSB supplemented with 5 mM EGTA, respectively, incubated at 26°C for 2 h, and then shifted to 37°C for 3 h to induce type III secretion. When appropriate, IPTG was added to a final concentration of 1 mM to induce the expression of plasmid-borne *lcrV* alleles. Cultures were fractionated and analyzed for type III secretion as described previously (32). To screen for *Yersinia* type III translocation of effectors, overnight cultures of *Y. pestis* and *Y. enterocolitica* were diluted 1:40 into 4 ml HIB or TSB, respectively, and incubated for 2 h at 26°C. Bacteria were added at a multiplicity of infection (MOI) of 10 to HeLa cell monolayers of about 2×10^5 cells that had been seeded a day earlier. After 3 h of infection at 37°C, cells were fixed with 3.7% formaldehyde for 20 min, quenched with 0.1 M glycine for 5 min, washed with phosphate-buffered saline (PBS), permeabilized with 0.1% Triton X-100 for 30 min at 4°C, washed three times with PBS, and blocked with 5% nonfat dried milk in PBS for 20 min at room temperature. Filamentous actin was then labeled with 3 units of rhodamine-conjugated phalloidin (99 nM) for 20 min. After the labeling solution was removed, the cells were washed three times with PBS and visualized by phase-contrast imaging and fluorescence microscopy using a Nikon TE-2000 inverted microscope (33).

Purification of LcrV from *Yersinia* extracts. To assay for cytosolic protein-protein interactions, 50 ml of overnight cultures of *Y. pestis* or *Y. enterocolitica* was inoculated into 1 liter of HIB supplemented with 20 mM $MgCl_2$ and 20 mM sodium oxalate or TSB supplemented with 5 mM EGTA, respectively. Cultures were incubated at 26°C for 2 h and then grown at 37°C for another 3 h. IPTG, at a final concentration of 1 mM, was added prior to the temperature shift to induce expression of plasmid-borne LcrV. Bacteria were sedimented by centrifugation at 7,500 × *g* for 10 min, suspended in 20 ml of column buffer (100 mM Tris-HCl, 150 mM NaCl [pH 7.5]), and left at −20°C overnight. The cells were thawed the following day and French pressed twice at 15,000 lb/in^2. The crude lysate was centrifuged twice at 8,000 × *g* for 15 min, and the supernatant (load) was subjected to chromatography on 1.5 ml of Strep-Tactin Sepharose (IBA BioTAGnology). The column was washed with 30 ml of column buffer, and the proteins were eluted with column buffer with 2.5 mM desthiobiotin. Samples were analyzed by 15% SDS-PAGE, Coomassie staining, or immunoblotting with rabbit antisera raised against purified recombinant *Yersinia* proteins or mouse monoclonal antibody directed against the Strep tag.

Purification and visualization of type III needles. Needle purification was carried out by inoculation of a 50-ml overnight culture of *Y. enterocolitica* into 1 liter of M9-Ca medium, which was incubated at 26°C for 2 h and then grown at 37°C for 3 h. LcrV expression was induced by the addition of 1 mM IPTG prior to incubation at 37°C. Bacteria were sedimented by centrifugation at 2,700 × *g* for 10 min and suspended in 40 ml of 1 M Tris-HCl (pH 7.5). Needles on the bacterial surface were mechanically sheared by vortexing the samples for 5 min. Bacteria were again sedimented by centrifugation at 8,000 × *g* for 10 min, and the needle containing shearate was passed through a 0.45-μm cellulose acetate membrane filter (Whatman). Needles were sedimented by ultracentrifugation at 45,000 × *g* for 30 min. The needle sediment was suspended in 20 mM Tris-HCl (pH 7.5) and examined by either immunoblotting or electron microscopy. For electron microscopy, all samples were placed on a carbon-coated copper grid and stained with 1% uranyl acetate before viewing on a Tecnai F30 electron microscope at 300 kV.

RESULTS

Mutations in *lcrV* with a dominant negative LCR^- phenotype in *Y. pestis*. *Y. pestis* $lcrV_{D27}$ was subjected to PCR mutagenesis, introducing mutations at frequencies ranging from 1 to 10 lesions per kilobase. Mutated plasmids were purified and transformed into wild-type *Y. pestis* strain KIM D27. Transformants were spread on agar with chelated calcium ions and incubated for 2 days at 37°C in the presence of 1 mM IPTG to induce the expression of plasmid-borne *lcrV*. Under these conditions, *Y. pestis* variants that lost the ability to secrete effectors formed colonies (20); these colonies were isolated, and the plasmids were purified and transformed again into *Y. pestis* KIM D27. Transformants that retained the LCR^- phenotype on calcium-chelated agar supplemented with 1 mM IPTG were analyzed by DNA sequencing of

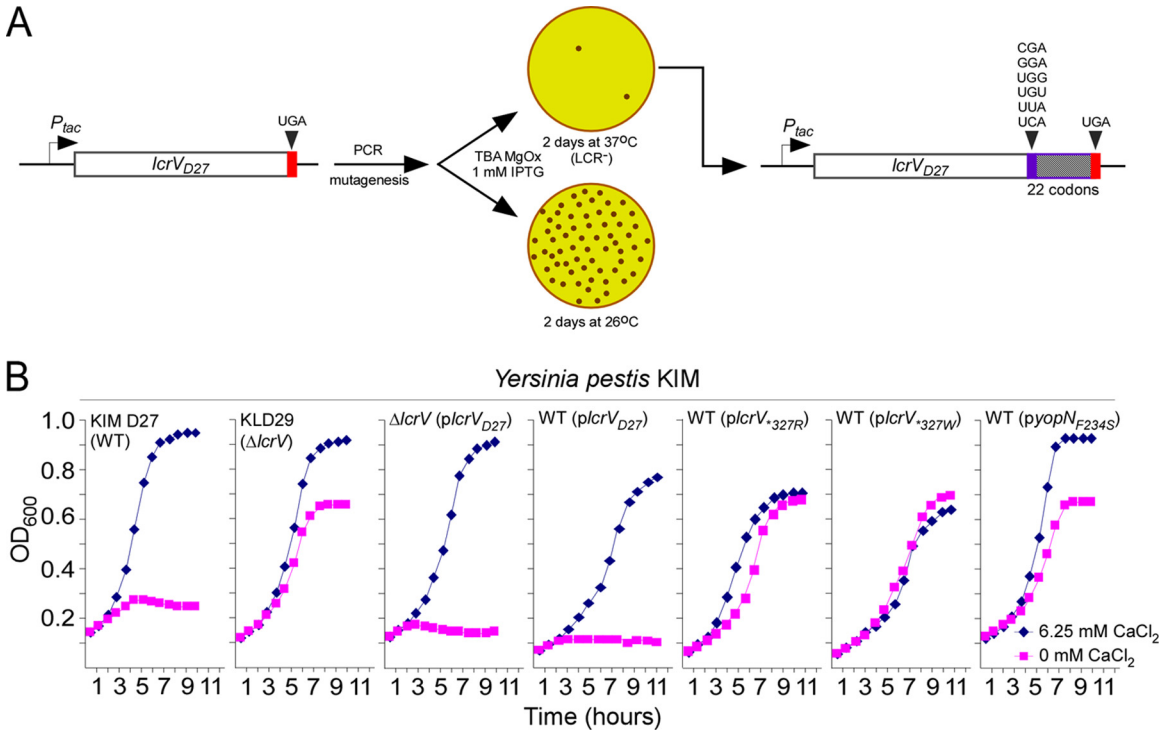

FIG 1 *Yersinia pestis lcrV* mutants with the dominant negative low-calcium response (LCR$^-$) phenotype. (A) $lcrV_{D27}$ was subjected to PCR mutagenesis, cloned under the control of the pHSG576 *tac* promoter, and electroporated into *Y. pestis* strain KIM D27. Transformants were quantified after colony formation on TBA supplemented with magnesium oxalate (MgOx) at 26°C or 37°C, at the latter temperature with selection for dominant negative LCR$^-$ mutants. Plasmids were isolated and again electroporated into *Y. pestis* strain KIM D27, growth of cells with the LCR$^-$ phenotype was verified, and plasmids were sequenced, which identified 18 mutations with missense mutations in codon 327 (UGA). These mutations extend the *lcrV* open reading frame by 22 codons (GSKQGGSVSPFF YQYCEYLRP*). (B) *Y. pestis* strains KIM D27 (wild-type [WT] *lcrV*) or KLD29 (Δ*lcrV*) harboring either no plasmid or p$lcrV_{D27}$, p$lcrV_{*327W}$, and p$lcrV_{*327R}$ were cultured at 37°C in TMH medium supplemented with either 0 mM or 6.25 mM $CaCl_2$. Growth was recorded as an increase in the optical density at 600 nm (OD_{600}). p$yopN_{F234S}$, which has been reported to cause a dominant negative LCR$^-$ phenotype (34), was used as a control.

plasmid-borne *lcrV*. Eighty-seven independent mutants were isolated, 18 of which harbored missense mutations in codon 327 (UGA amber stop), extending the $lcrV_{D27}$ reading frame by 22 codons (Fig. 1A). Specifically, we identified 6 CGA (Arg), 2 GGA (Gly), 3 UGG (Trp), 2 UGU (Cys), 4 UUA (Lys), and 1 UCA (Ser) codon variants. The remaining mutants that answered the selection were stop or frameshift mutations at various locations throughout the *lcrV* gene.

Y. pestis KIM D27 strains harboring plasmids expressing wild-type $lcrV_{D27}$ (p$lcrV_{D27}$) or the amber codon suppressors (p$lcrV_{*327R}$ and p$lcrV_{*327W}$) were grown in liquid media at 37°C for 12 h under secretion-permissive (TMH medium) or secretion-nonpermissive conditions (TMH medium supplemented with 2.5 mM $CaCl_2$) (Fig. 1B). In contrast to the plasmid expressing $lcrV_{D27}$, p$lcrV_{*327R}$ and p$lcrV_{*327W}$ enabled IPTG-induced *Y. pestis* cultures to grow at 37°C in the absence of calcium ions (LCR$^-$) (Fig. 1B). As controls, *Y. pestis* KIM D27 without plasmid was LCR$^+$, whereas p$yopN_{F234S}$ resulted in the expected dominant negative LCR$^-$ phenotype (34) (Fig. 1B). Deletion of the *lcrV* gene on pCD1 from *Y. pestis* KIM D27 also caused an LCR$^-$ phenotype, as the Δ*lcrV* mutant strain (KLD29) continued to grow at 37°C in the absence of calcium; this defect was complemented by the transformation of KLD29 with p$lcrV_{D27}$ (Fig. 1B).

Y. pestis strains were grown in liquid media for 2 h at 26°C and then shifted to 37°C for 3 h to induce type III secretion. The cultures were centrifuged to separate the extracellular medium with the supernatant from the bacterial sediment. Proteins in both fractions were analyzed by immunoblotting with rabbit antisera raised against purified LcrV, YopE, or RNA polymerase subunit A (RpoA) (Table 1). *Y. pestis* strain KIM D27 (p$lcrV_{D27}$) secreted LcrV and YopE into the extracellular medium, whereas RpoA was found only in the bacterial sediment. As expected, the Δ*lcrV* mutant did not express LcrV and failed to secrete YopE, which was

TABLE 1 Missense mutations in *lcrV* codon 327 block *Yersinia pestis* type III secretion

Y. pestis strain	Plasmid	% type III secretion ([S]/[S+P])[a]	
		YopE	LcrV
KIM D27 (wild type)	p$lcrV_{D27}$	36.6	28.3
KIM D27 (wild type)	p$lcrV_{*327R}$	1.3	12.6
KIM D27 (wild type)	p$lcrV_{*327W}$	1.2	10.3
KLD29 (Δ*lcrV*)	None	1.7	ND[b]
KLD29 (Δ*lcrV*)	p$lcrV_{D27}$	33.2	36.2

[a] Type III secretion of *Y. pestis* was measured after 3 h of growth in cultures that were grown in media with chelated calcium ions at 37°C. Following centrifugation, the extracellular medium was separated into the supernatant (S) and the bacterial pellet (P), and proteins in both fractions were precipitated with trichloroacetic acid and analyzed by immunoblotting with specific antibodies against the type III secretion substrates YopE and LcrV. Secretion was quantified by calculating the percent amount of secreted protein [S] derived from protein in both the medium and the pellet [S+P].
[b] ND, no immunoreactive signal detected.

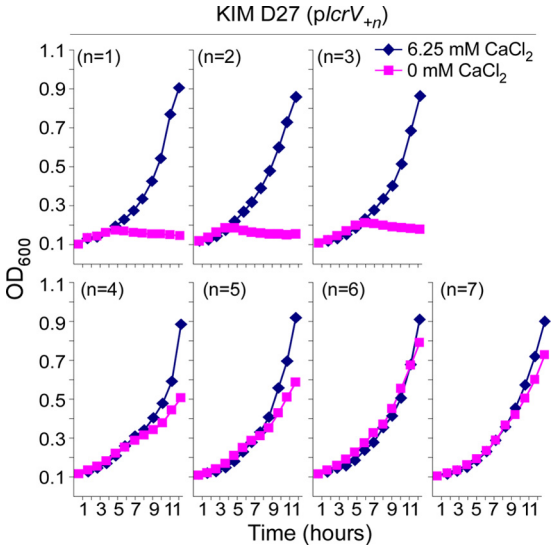

FIG 2 Short extensions at the C terminus of LcrV cause a dominant negative LCR$^-$ phenotype in *Y. pestis*. The open reading frame of $lcrV_{D27}$ was extended by single-codon insertions at position 327, immediately prior to the UGA stop codon. *Y. pestis* strain KIM D27 harboring p$lcrV_{+1}$, p$lcrV_{+2}$, p$lcrV_{+3}$, p$lcrV_{+4}$, p$lcrV_{+5}$, p$lcrV_{+6}$, or p$lcrV_{+7}$ was cultured at 37°C in TMH medium supplemented with either 0 mM or 6.25 mM $CaCl_2$. Growth was recorded as an increase in the OD_{600}.

again complemented by p$lcrV_{D27}$ (Table 1). *Y. pestis* KIM D27 harboring p$lcrV_{*327R}$ or p$lcrV_{*327W}$ failed to secrete YopE yet retained the ability to secrete mutant LcrV$_{*327R}$ and LcrV$_{*327W}$, albeit at reduced abundance (Table 1). Together, these data indicate that the IPTG-inducible expression of $lcrV_{*327R}$ and $lcrV_{*327W}$ causes a dominant negative LCR$^-$ phenotype in *Y. pestis* strain KIM D27. This is attributable to a type III secretion block of $lcrV_{*327R}$ and $lcrV_{*327W}$ mutants for effector Yops, whereas the secretion of LcrV was reduced but not blocked.

C-terminal extensions of LcrV block the *Y. pestis* type III pathway. We wondered whether the LCR$^-$ phenotype of the $lcrV_{*327R}$ and $lcrV_{*327W}$ mutants critically depended on the 22 codons downstream of their stop codon suppressors. To test this, we extended the $lcrV_{D27}$ open reading frame by insertions of random single amino acid codons immediately prior to codon 327 (UGA). The resulting variants were expressed from plasmids via IPTG induction of the lac_{UV5} promoter. Expression of *lcrV* alleles with one (p$lcrV_{+1}$), two (p$lcrV_{+2}$), or three codon insertions (p$lcrV_{+3}$) did not affect bacterial growth; however, *lcrV* alleles with four (p$lcrV_{+4}$), five (p$lcrV_{+5}$), six (p$lcrV_{+6}$), or seven (p$lcrV_{+7}$) codon insertions abolished the LCR of *Y. pestis* strain KIM D27 (Fig. 2). These data indicate that the mere extension of *Y. pestis* LcrV by four or more residues at its C-terminal end is sufficient to impose a dominant negative blockade on the type III pathway.

Strep tag insertions into *Y. enterocolitica* LcrV. Earlier work revealed that LcrV caps the tip of *Y. enterocolitica* needles (11). As details regarding *Y. pestis* needles and their LcrV caps have not yet been revealed (35), we sought to examine the cap structure and other functional attributes of *lcrV* alleles in *Y. enterocolitica* W22703 (1, 31). LcrV$_{W22703}$ is three residues shorter than LcrV$_{D27}$; however, the two molecules are 96% identical (Fig. 3A). To generate a C-terminal extension of LcrV$_{W22703}$, we appended the eight-residue Strep tag to the C-terminal end of the polypeptide chain by inserting the corresponding eight codons immediately upstream of the $lcrV_{W22703}$ stop codon (p$lcrV_{S324}$). Furthermore, we wondered whether Strep tag insertions at other sites also cause a dominant negative type III secretion (LCR) phenotype, and we selected LcrV$_{W22703}$ positions 1, 20, 55, 170, 228, and 270 for insertions. The relative positions of these insertions in the three-dimensional structure of LcrV$_{K40A/D41A/K42A}$ and their corresponding phenotypes are summarized in Fig. 3B. Plasmids expressing $lcrV_{W22703}$ or its variants via the lac_{UV5} promoter were transformed into *Y. enterocolitica* CT1, the Δ*lcrV* variant of W22703. In contrast to *Y. pestis*, where the deletion of *lcrV* abolished the LCR and type III secretion, *Y. enterocolitica* CT1 (Δ*lcrV*) remains competent for both YopE expression and type III secretion (Fig. 3C) (17). Of note, LcrG, the cytoplasmic chaperone of LcrV, is expressed at very low abundance in the *lcrV* mutant strain (Fig. 3C) (17). Transformation of *Y. enterocolitica* CT1 with p$lcrV_{W22703}$ restored the expression of both LcrV$_{W22703}$ and LcrG and enabled the secretion of LcrV$_{W22703}$ (Fig. 3C). Similar phenotypes were observed with p$lcrV_{S1}$, p$lcrV_{S20}$, p$lcrV_{S55}$, p$lcrV_{S170}$, and p$lcrV_{S228}$. The p$lcrV_{S270}$ plasmid did not restore the expression of LcrG, and LcrV$_{S270}$ was not secreted into the extracellular medium. Plasmid p$lcrV_{S324}$ restored the expression of LcrG, and only very small amounts of LcrV$_{S324}$ were secreted into the extracellular medium (Fig. 3C).

To analyze the binding of LcrV mutants to LcrG, extracts of *Y. enterocolitica* CT1 harboring *lcrV* plasmids were subjected to affinity chromatography on Strep-Tactin Sepharose. Cleared lysate (L) and eluate (E) were analyzed by Coomassie blue-stained SDS-PAGE and immunoblotting (Fig. 4). LcrV$_{S1}$, LcrV$_{S20}$, LcrV$_{S55}$, LcrV$_{S228}$, and LcrV$_{S324}$ were isolated by affinity chromatography and purified together with LcrG (Fig. 4). LcrV$_{S170}$ did not bind Strep-Tactin resin, and the Strep tag was only poorly recognized by a specific monoclonal antibody. We therefore conclude that the Strep tag of LcrV$_{S170}$ may be buried within the polypeptide and inaccessible to either antibody or Strep-Tactin (Fig. 4). LcrV$_{S270}$ was purified from *Yersinia* lysate; however, this protein cannot copurify with LcrG, as the chaperone is not expressed by *Y. enterocolitica* CT1 harboring p$lcrV_{S270}$ (Fig. 4). Thus, with the exception of LcrV$_{S270}$, all other variants do bind to their LcrG chaperone.

To assess the functions of *lcrV* alleles in needle cap assembly and injectisome functions, we measured *Y. enterocolitica* effector translocation into tissue culture cells. HeLa cells were infected with *Y. enterocolitica* CT1 expressing mutant *lcrV*. Phase-contrast microscopy and fluorescence microscopy images of phalloidin-stained tissue cultures were used to reveal actin filament rearrangements and cell rounding as measures for *Yersinia* type III translocation of effectors (5) (see Fig. S1 in the supplemental material). Of note, p$lcrV_{S1}$, p$lcrV_{S20}$, p$lcrV_{S55}$, and p$lcrV_{S228}$ enabled *Y. enterocolitica* CT1 (Δ*lcrV*) to inject effectors, whereas p$lcrV_{S170}$, p$lcrV_{S270}$, and p$lcrV_{S324}$ did not (see Fig. S1). When transformed into wild-type *Y. enterocolitica* W22703, only p$lcrV_{S324}$ caused a dominant negative effect on type III effector translocation, while p$lcrV_{S1}$, p$lcrV_{S20}$, p$lcrV_{S55}$, p$lcrV_{S170}$, p$lcrV_{S228}$, and p$lcrV_{S270}$ had no effect (see Fig. S1). These data indicate that the C-terminal extension of LcrV$_{W22703}$ in *Y. enterocolitica* $lcrV_{S324}$ blocked the type III secretion pathway similarly to $lcrV_{*327W}$, $lcrV_{*327R}$, and $lcrV_{S324}$ in *Y. pestis*. Further, Strep tag insertions at positions 170 and 270 abolished the ability of LcrV$_{S170}$ and LcrV$_{S270}$ to assemble the type III injectisome and translocate effectors. For LcrV$_{S270}$,

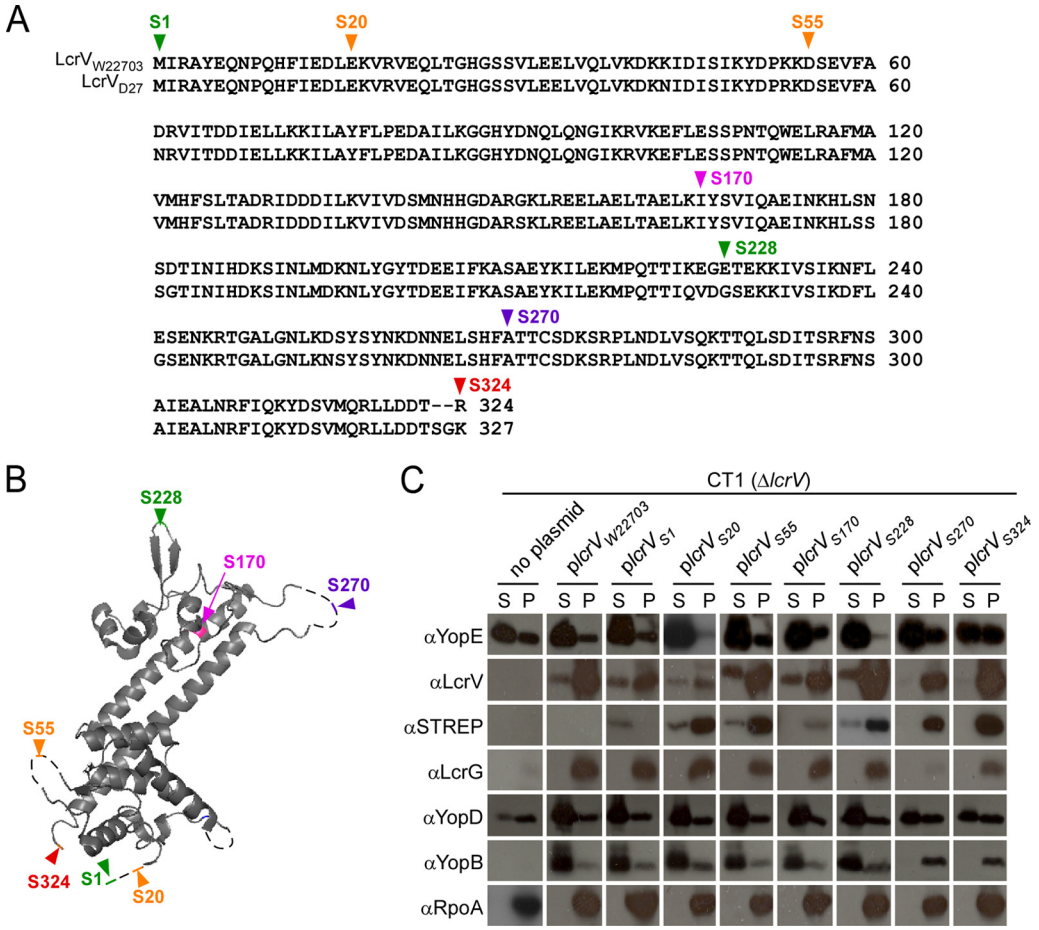

FIG 3 Strep tag insertions in LcrV. (A) Alignment of amino acid sequences derived from the *lcrV* gene of *Y. enterocolitica* strain W22703 (LcrV$_{W22703}$) or *Y. pestis* strain KIM D27 (LcrV$_{D27}$). LcrVs derived from *Y. enterocolitica* and *Y. pestis* were aligned. Arrowheads and S numbers identify the amino acids (codons) where the Strep tag (NH_2-WSHPQFEK-COOH) was inserted into LcrV$_{W22703}$. (B) Ribbon diagram illustrating the three-dimensional X-ray structure of LcrV (28) and the positions of the Strep tags. LcrV$_{S1}$ and LcrV$_{S228}$ (green) displayed wild-type LcrV phenotypes in both *Y. enterocolitica* and *Y. pestis*. LcrV$_{S270}$ (blue) was nonfunctional, and LcrV$_{S324}$ (red) caused a dominant negative blockade of the type III pathway in both *Y. enterocolitica* and *Y. pestis*. LcrV$_{S20}$ and LcrV$_{S55}$ (both orange) caused a dominant negative blockade of type III secretion only in *Y. pestis* and not in *Y. enterocolitica*. Finally, LcrV$_{S170}$ (purple) did not affect type III secretion *in vitro* but failed to promote effector translocation for both *Y. enterocolitica* and *Y. pestis*. (C) *Y. enterocolitica* CT1 (Δ*lcrV* variant of W22703) without plasmid or harboring p*lcrV*$_{W22703}$, p*lcrV*$_{S1}$, p*lcrV*$_{S20}$, p*lcrV*$_{S55}$, p*lcrV*$_{S170}$, p*lcrV*$_{S228}$, p*lcrV*$_{S270}$, or p*lcrV*$_{S324}$ was grown for 3 h at 37°C in TSB supplemented with 5 mM EGTA to chelate calcium and 1 mM IPTG to induce the expression of plasmid-borne *lcrV* alleles. *Yersinia* cultures were centrifuged, and the extracellular medium was removed with the supernatant (S) and separated from the bacterial sediment (pellet [P]). Proteins in both fractions were precipitated with trichloroacetic acid and analyzed by immunoblotting with rabbit antisera raised against YopE (αYopE), LcrV (αLcrV), YopB (αYopB), YopD (αYopD), LcrG (αLcrG), or RpoA (αRpoA) or a monoclonal antibody specific for the Strep tag (αStrep).

this is attributable to a defect in binding and stabilizing LcrG, which results in a defect in the type III secretion of LcrV$_{S270}$.

LcrV$_{S228}$ and LcrV$_{S324}$ cap *Y. enterocolitica* type III needles. We sought to determine whether LcrV$_{S324}$ can cap type III needle structures. *Y. enterocolitica* CT1 (Δ*lcrV*) without plasmid or with p*lcrV*$_{W22703}$, p*lcrV*$_{S228}$, or p*lcrV*$_{S324}$ was sheared to remove type III secretion needles, which were subsequently sedimented by ultracentrifugation. Electron microscopy experiments revealed the absence of a cap structure on *Y. enterocolitica* Δ*lcrV* needles (Fig. 5A). Plasmids p*lcrV* and p*lcrV*$_{S228}$, as well as p*lcrV*$_{S324}$, restored the assembly of the LcrV cap on YscF needles (Fig. 5B). To examine whether capped needles also copurify with the injectisome component YopD, needle preparations were subjected to immunoblotting (11, 36). As expected, needles derived from *Yersinia* with p*lcrV*$_{W22703}$ or p*lcrV*$_{S228}$ were assembled from YscF, YopD, and LcrV, whereas the needle preparations from the Δ*lcrV* mutant harbored YscF, very little YopD, and no LcrV. In contrast, needles from *Y. enterocolitica* Δ*lcrV* (p*lcrV*$_{S324}$) were assembled from YscF and LcrV$_{S324}$; however, the structures lacked YopD (Fig. 5B). Taken together, these data suggest that LcrV$_{S324}$ can indeed cap the type III needle. In contrast to wild-type LcrV or LcrV$_{S228}$, LcrV$_{S324}$-capped needles lack YopD, which may explain the effector translocation defect of the *lcrV*$_{S324}$ mutant strain. Electron microscopy experiments have not yet positioned YopD within the capped-needle complex. The finding that LcrV$_{S228}$-capped needles, but not the nonfunctional LcrV$_{S324}$ cap, associate with YopD provides evidence for a model whereby specific interactions between YscF, LcrV, and YopD promote the formation of capped needles that eventually progress toward injectisome assembly.

Phenotypes of Strep-tagged LcrV expressed in *Y. pestis*. Subtle differences between the type III pathways of *Y. enterocolitica* and *Y. pestis* have been reported (37). First, *Y. pestis*, but not *Y.*

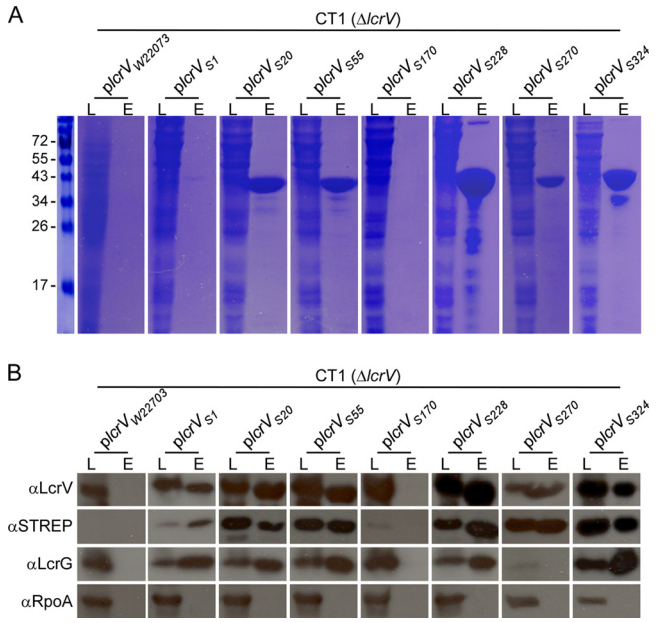

FIG 4 Affinity chromatography of Strep-tagged LcrV. (A) Cleared lysates of *Y. enterocolitica* CT1 (Δ*lcrV*) harboring p*lcrV*$_{W22703}$ or Strep-tagged LcrV (p*lcrV*$_{S1}$, p*lcrV*$_{S20}$, p*lcrV*$_{S55}$, p*lcrV*$_{S170}$, p*lcrV*$_{S228}$, p*lcrV*$_{S270}$, and p*lcrV*$_{S324}$) were derived from cultures grown for 3 h at 37°C in TSB supplemented with 5 mM EGTA to chelate calcium and 1 mM IPTG to induce the expression of plasmid-borne *lcrV* alleles. Cleared lysates (L) were subjected to affinity chromatography on Strep-Tactin resin and eluted with desthiobiotin (E). Proteins in both samples were analyzed by Coomassie blue-stained SDS-PAGE. The migratory positions were proteins with known molecular mass (in kDa, indicated on the left). (B) Samples were subjected to immunoblotting with rabbit antisera raised against LcrV (αLcrV), LcrG (αLcrG), and RpoA (αRpoA) or with monoclonal antibody against the Strep tag (αStrep).

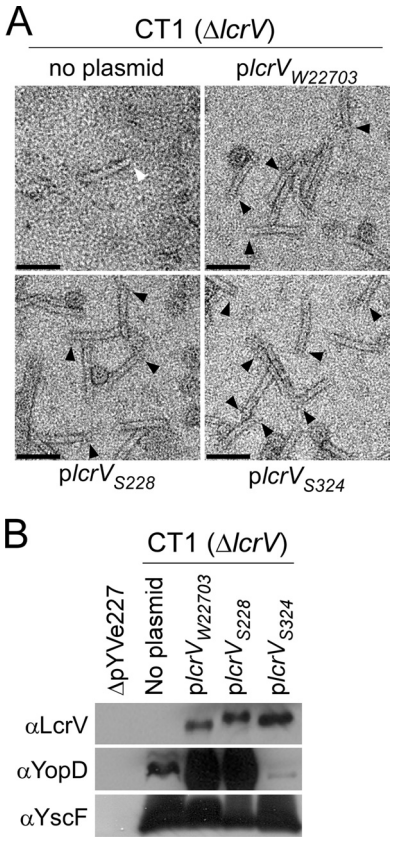

FIG 5 LcrV$_{S324}$ caps YscF needles that lack YopD. (A) Cultures of *Y. enterocolitica* CT1 (Δ*lcrV*) harboring p*lcrV*$_{W22703}$, p*lcrV*$_{S228}$, p*lcrV*$_{S324}$, or no plasmid were centrifuged, and the bacterial sediment was sheared to break off type III needle complexes. Bacteria were removed by slow-speed centrifugation, and the filtered supernatant was ultracentrifuged to sediment type III needle complexes, which were analyzed by transmission electron microscopy. The arrowheads identify LcrV caps of type III needle complexes. (B) *Y. enterocolitica* CT1 (Δ*lcrV*) and *Y. enterocolitica* ΔpYVe227 cultures were subjected to the isolation of type III needle complexes as described above. Samples were analyzed by immunoblotting with rabbit antisera raised against LcrV (αLcrV), YopD (αYopD), and YscF (αYscF).

enterocolitica, displays an LCR phenotype (20, 38). Thus, low-calcium-induced activation of type III secretion in *Y. enterocolitica* does not lead to complete growth restriction even though large amounts of effectors are secreted into the extracellular medium (39). Second, even though *lcrG* and *lcrV* encode nearly identical products in pathogenic *Yersinia*, mutations in these genes cause different phenotypes. Deletion of *Y. pestis lcrG* causes a calcium-blind phenotype, whereas deletion of *lcrV* results in an LCR$^-$ phenotype, whereby the type III secretion of effectors is abolished even when bacteria are incubated in the absence of calcium (23, 24). In contrast, the deletion of *Y. enterocolitica lcrV* does not abrogate low-calcium-induced type III secretion of effectors (17). These differences cannot be explained by the amino acid polymorphisms of *lcrV* products, as the expression of *lcrV*$_{W22703}$ in *Y. pestis* or *lcrV*$_{D27}$ in *Y. enterocolitica* results in wild-type phenotypes (33). The deletion of *Y. enterocolitica lcrG* causes a class I secretion phenotype (40); although *Y. enterocolitica lcrG* mutants continue to grow, the variants secrete all effectors in both the presence and absence of calcium (17, 41).

To test whether *lcrV* alleles isolated here displayed different phenotypes in *Y. enterocolitica* and *Y. pestis*, plasmids p*lcrV*$_{S1}$, p*lcrV*$_{S20}$, p*lcrV*$_{S55}$, p*lcrV*$_{S170}$, p*lcrV*$_{S228}$, p*lcrV*$_{S270}$, and p*lcrV*$_{S324}$ were also transformed into *Y. pestis* strains KIM D27 and KLD29 (Δ*lcrV*). When analyzed for growth in the presence or absence of calcium, plasmids p*lcrV*$_{S1}$, p*lcrV*$_{S170}$, and p*lcrV*$_{S228}$ restored the LCR$^-$ phenotype of *Y. pestis* stain KLD29 (Δ*lcrV*) to LCR$^+$, whereas p*lcrV*$_{S20}$, p*lcrV*$_{S55}$, p*lcrV*$_{S270}$, and p*lcrV*$_{S324}$ did not (Fig. 6). Further, p*lcrV*$_{S1}$, p*lcrV*$_{S170}$, and p*lcrV*$_{S228}$ complemented the type III secretion defect of the Δ*lcrV* mutant, whereas p*lcrV*$_{S270}$ and p*lcrV*$_{S324}$ blocked the secretion of both YopE and LcrV$_{S270}$ or LcrV$_{S324}$ (Table 2). Two *lcrV* plasmids produced different phenotypes in *Y. pestis* and *Y. enterocolitica*. Plasmids p*lcrV*$_{S20}$ and p*lcrV*$_{S55}$ caused a dominant negative LCR$^-$ and effector translocation phenotype in *Y. pestis* (Fig. 6) and reduced the type III secretion of YopE (Table 2). In contrast, p*lcrV*$_{S20}$ and p*lcrV*$_{S55}$ complemented the type III secretion and effector translocation defects of the *Y. enterocolitica lcrV* mutant. In comparison with p*lcrV*$_{S20}$ and p*lcrV*$_{S55}$, p*lcrV*$_{S324}$ caused a stronger LCR$^-$ phenotype in *Y. pestis* strain KIM D27 and abolished the type III secretion of YopE, similar to the effects on *lcrV*$_{*327W}$ and *lcrV*$_{*327R}$ (Tables 1 and 2).

As with data obtained with *Y. enterocolitica*, affinity chromatography of Strep-tagged LcrV on Strep-Tactin resin revealed the copurification of LcrV$_{S1}$, LcrV$_{S20}$, LcrV$_{S55}$, LcrV$_{S228}$, and LcrV$_{S324}$ with LcrG (see Fig. S2 in the supplemental material). As LcrG is not expressed in *Y. pestis* KLD29 (p*lcrV*$_{S270}$), LcrV$_{S270}$ did not

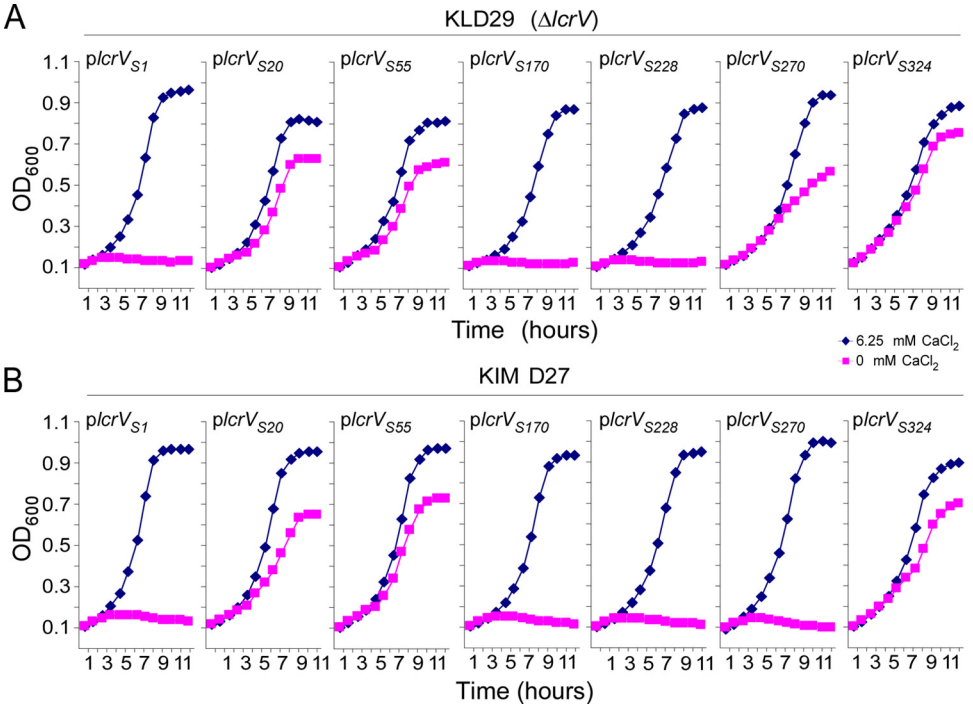

FIG 6 Strep-tagged LcrVs and their LCR phenotypes in *Yersinia pestis*. (A) *Y. pestis* KLD29 (Δ*lcrV*) expressing Strep-tagged LcrV (p*lcrV*$_{S1}$, p*lcrV*$_{S20}$, p*lcrV*$_{S55}$, p*lcrV*$_{S170}$, p*lcrV*$_{S228}$, p*lcrV*$_{S270}$, and p*lcrV*$_{S324}$) was cultured at 37°C in TMH medium supplemented with either 0 mM or 6.25 mM $CaCl_2$. Growth was recorded as an increase in the OD_{600}. (B) *Y. pestis* strain KIM D27 (wild-type *lcrV*) expressing Strep-tagged LcrV (p*lcrV*$_{S1}$, p*lcrV*$_{S20}$, p*lcrV*$_{S55}$, p*lcrV*$_{S170}$, p*lcrV*$_{S228}$, p*lcrV*$_{S270}$, and p*lcrV*$_{S324}$) was cultured at 37°C in TMH medium supplemented with either 0 mM or 6.25 mM $CaCl_2$. Growth was recorded as an increase in the OD_{600}.

copurify with LcrG. GST-LcrG was purified from the cytoplasm of *Escherichia coli* using affinity chromatography on glutathione-Sepharose (17). GST-LcrG binding to $LcrV_{S228}$, $LcrV_{S170}$, or $LcrV_{S270}$ was analyzed via chromatography of *Yersinia* lysates and immunoblotting; GST-LcrG retained $LcrV_{S228}$ and $LcrV_{170}$ but not $LcrV_{S270}$ (see Fig. S2). As a control, YopB harboring a Strep tag at the N terminus was not retained during GST-LcrG chromatography (see Fig. S2). These data indicate that LcrV binding is required for LcrG expression. Presumably, LcrG that is not bound to LcrV is rendered unstable and may be degraded by *Yersinia*.

TABLE 2 Insertions of the eight-codon Strep tag at various positions into *lcrV* and its effect on *Yersinia pestis* type III secretion of YopE or LcrV

	% type III secretion ([S]/[S+P])[a]			
	KIM D27 (wild type)		KLD29 (Δ*lcrV*)	
Plasmid	YopE	LcrV	YopE	LcrV
None	47.1	21.3	3.7	ND[b]
p*lcrV*$_{W22703}$	50.3	37.8	51.1	31.8
p*lcrV*$_{S1}$	52.3	25.8	60.8	24.1
p*lcrV*$_{S20}$	4.6	16.8	7.7	22.7
p*lcrV*$_{S55}$	4.1	15.8	13.2	21.9
p*lcrV*$_{S170}$	48.4	39.7	45.6	36.3
p*lcrV*$_{S228}$	49.2	38.9	63.4	37.6
p*lcrV*$_{S270}$	54.1	38.5	2.8	1.1

[a] Type III secretion of *Y. pestis* strains without or with *lcrV* plasmids was measured after 3 h of growth in cultures that were grown in media with chelated calcium ions at 37°C. Following centrifugation, the extracellular medium was separated into the supernatant (S) and the bacterial pellet (P), and proteins in both fractions were precipitated with trichloroacetic acid and analyzed by immunoblotting with specific antibodies against the type III secretion substrates YopE and LcrV. Secretion was quantified by calculating the percent amount of secreted protein [S] compared to protein in both the medium and the pellet [S+P].

[b] ND, no immunoreactive signal detected.

When analyzed for the type III injection of effectors into HeLa cells, *Y. pestis* strain KIM D27 with or without p*lcrV*$_{W22703}$ caused actin cable rearrangements and cell rounding (Fig. 7). Plasmids p*lcrV*$_{S1}$ and p*lcrV*$_{S228}$ did not affect the ability of *Y. pestis* KIM D27 type III machines to translocate effectors, whereas p*lcrV*$_{S170}$, p*lcrV*$_{S270}$, and p*lcrV*$_{S324}$ caused a dominant negative blockade of the *Y. pestis* type III pathway (Fig. 7). Of note, we observed an intermediate type III effector translocation phenotype for p*lcrV*$_{S20}$ and p*lcrV*$_{S55}$ (Fig. 7). When transformed into *Y. pestis* strain KLD29 (Δ*lcrV*), p*lcrV*$_{W22703}$, p*lcrV*$_{S1}$, and p*lcrV*$_{S228}$ complemented the type III injection phenotype, whereas p*lcrV*$_{S170}$, p*lcrV*$_{S270}$, and p*lcrV*$_{S324}$ did not. In contrast to *Y. enterocolitica*, expression of *lcrV*$_{S20}$ or *lcrV*$_{S55}$ in the *Y. pestis* Δ*lcrV* mutant did not restore function for the type III pathway (Fig. 7).

$LcrV_{S324}$ blocks the calcium-blind phenotype of *Y. pestis yscF* needle mutants. Earlier work revealed that *Y. pestis* YP517 *yscF*$_{D28A}$, *yscF*$_{D46A}$, and *yscF*$_{D28A,D46A}$ mutants display a calcium-blind growth phenotype and secrete effectors constitutively when bacteria are grown at 37°C. IPTG-induced expression of *lcrV*$_{S324}$ blocked the calcium-blind phenotype of *yscF*$_{D28A}$, *yscF*$_{D46A}$, and *yscF*$_{D28A,D46A}$ mutants, imposing an LCR^- blockade on the type III pathway (Fig. 8 and Table 3). As a control, the expression of *lcrV*$_{S324}$ did not affect the growth of *yscF*$_{D77A}$ LCR^- mutants. When we analyzed for type III secretion, we found that the expression of *lcrV*$_{S324}$ blocked the secretion of YopH in *yscF*$_{D28A}$,

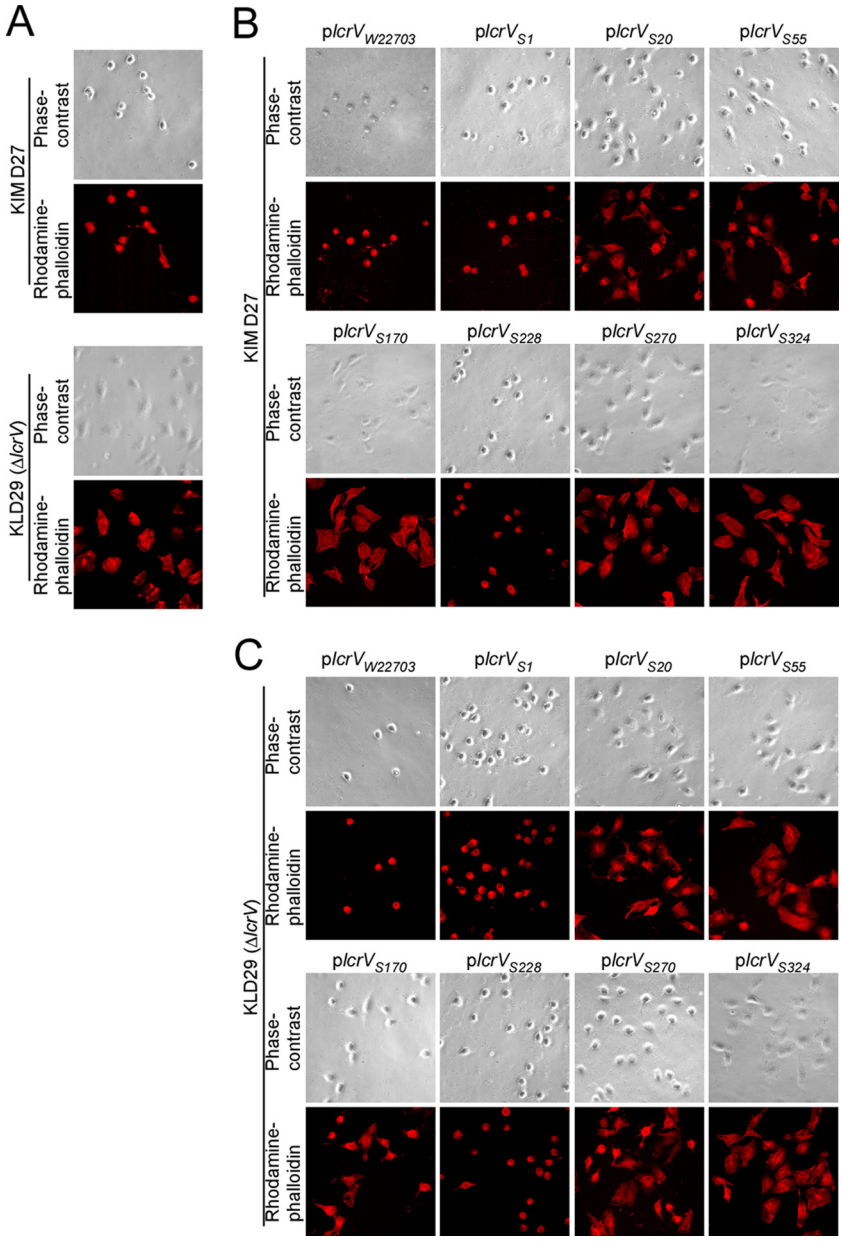

FIG 7 Strep-tagged LcrV and *Yersinia pestis* effector translocation. (A) *Y. pestis* strains KIM D27 (wild-type *lcrV*) and KLD29 (Δ*lcrV*) were used to infect HeLa tissue culture cells for 3 h at an MOI of 10. Samples were fixed, stained with rhodamine-phalloidin, and imaged by fluorescence or phase-contrast microscopy to reveal actin cable rearrangements and cell rounding as a measure for effector translocation. (B) *Y. pestis* KIM D27 strains harboring *lcrV* plasmids (p*lcrV*$_{W22703}$, p*lcrV*$_{S1}$, p*lcrV*$_{S20}$, p*lcrV*$_{S55}$, p*lcrV*$_{S170}$, p*lcrV*$_{S228}$, p*lcrV*$_{S270}$, and p*lcrV*$_{S324}$) were subjected to the same assay as described for panel A. (C) *Y. pestis* KLD29 strains harboring *lcrV* plasmids (p*lcrV*$_{W22703}$, p*lcrV*$_{S1}$, p*lcrV*$_{S20}$, p*lcrV*$_{S55}$, p*lcrV*$_{S170}$, p*lcrV*$_{S228}$, p*lcrV*$_{S270}$, and p*lcrV*$_{S324}$) were subjected to the same assay as described for panel A.

yscF$_{D46A}$, and *yscF*$_{D28A,D46A}$ mutants but did not restore the ability of the *yscF*$_{D77A}$ variant to secrete YopH (Table 3).

DISCUSSION

LcrV is the protective antigen of *Y. pestis*, and subunit vaccines that raise high-titer antibodies against this polypeptide confer protection against bubonic and pneumonic plague in mice, rats, guinea pigs, rabbits, cynomolgus macaques, and African Green monkeys (26, 42). Both *in vitro* and *in vivo* studies have indicated that LcrV antibodies block *Y. pestis* type III translocation of effectors into immune cells (27, 33). Studies with *Yersinia lcrV*, *yopB*, and *yopD* mutants suggest that these type III secretion substrates are each required for the translocation of effectors into host cells (17–19). Electron microscopy and biochemistry experiments revealed that the YscF needle of *Y. enterocolitica* is capped by LcrV and perhaps by YopD (11). Contact of the needle with host cell membranes is thought to trigger the formation of the injectisome, a YopB-YopD complex that establishes a conduit across the plasma membrane of host cells (13, 43). Appreciation of the molecular details and the mechanistic features of this model is neces-

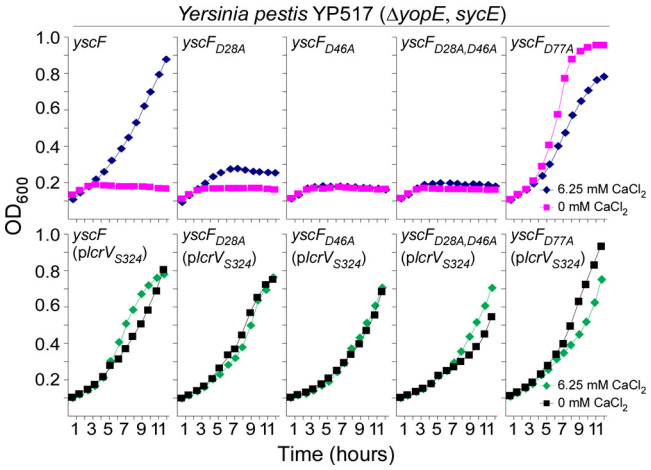

FIG 8 $LcrV_{S324}$ causes a dominant negative LCR^- phenotype in *Y. pestis* harboring calcium-blind alleles $yscF_{D28A}$ and/or $yscF_{D46A}$. (A) *Y. pestis* YP517 (Δ*yopE*/*sycE*) harboring wild-type *yscF*, the calcium-blind alleles $yscF_{D28A}$ and/or $yscF_{D46A}$, or the LCR^- $yscF_{D77A}$ allele were transformed with p$lcrV_{S324}$. Strains without (top panels) or with p$lcrV_{S324}$ (bottom panels) were cultured at 37°C in TMH medium supplemented with either 0 mM or 6.25 mM $CaCl_2$. Growth was recorded as an increase in the OD_{600}.

sary in order to understand why some, but certainly not all, antibodies against LcrV block effector translocation by the *Y. pestis* type III machine (34, 44). We reported recently that the ability of LcrV antibodies to block *Y. pestis* effector translocation does not extend to *Y. enterocolitica* type III machines and that the observed differences are not based on the amino acid polymorphisms in $LcrV_{W22703}$ and $LcrV_{D27}$ (33). These observations suggest that type III machines in *Y. pestis* and *Y. enterocolitica* have evolved discrete differences in injectisome assembly. Here, we used a genetic approach to initiate the analysis of LcrV features essential for injectisome assembly and effector translocation.

Exploiting *Y. pestis* LCR growth restriction, we isolated dominant negative *lcrV* mutants and observed that these variants harbored missense mutations in the amber codon at position 327, which extended the *lcrV* open reading frame by 22 codons. Neither the identity of the amino acids in the C-terminal extension nor its length appears to be critical for the type III blockade, as four or more residues with seemingly random sequences caused the same dominant negative LCR^- phenotype as the 22-residue extension. We achieved a similar effect by adding a C-terminal Strep tag to *Y. enterocolitica* strain W22703 and expressing $lcrV_{S324}$ in *Y. pestis*. The $LcrV_{S324}$ protein assembles as a cap on *Y. enterocolitica* YscF needles; however, the $LcrV_{S324}$-capped needles are not competent for effector translocation into HeLa cells. Unlike wild-type LcrV, $LcrV_{S324}$ needles lack YopD, suggesting that the C-terminal extension of LcrV may block the assembly of the injectisome. This assembly process appears to occur within the cap structure, as wild-type needles do not bind YopD antibodies and YopD antibodies cannot block effector translocation (45, 46). Further, needles capped by $LcrV_{S324}$ do not bind Strep-Tactin resin or Strep tag-specific antibodies, and these needles lack the YopD component of the injectisome. We propose a model whereby the LcrV cap of the type III needle not only interacts with YscF but also contributes to the recruitment of YopD into the injectisome.

YscF, the needle protein, is thought to function as a calcium sensor and may bind calcium ions via aspartyls 28 and 46 (21). *Y. pestis* type III machines harboring $YscF_{D28A,D46A}$ are calcium blind and secrete effectors even in the presence of millimolar concentrations of calcium ions, presumably because the mutant needle complexes assume the conformation of a fully activated type III pathway (21). The experiments illustrated in Fig. 8 demonstrate that the expression of $lcrV_{S324}$ in *Y. pestis* $yscF_{D28A,D46A}$ results in a dominant negative LCR^- phenotype and in the complete blockage of type III secretion. We surmise that $LcrV_{S324}$ is able to cap $YscF_{D28A,D46A}$ needles and lock the secretion machine in a conformation representing an inactive assembly intermediate. Such a model allows us to derive several predictions. First, $lcrV_{S324}$ may exert a dominant negative phenotype for other calcium-blind mutants capable of $LcrV_{S324}$ secretion, which may include the *yopN*, *tyeA*, *sycN*, and *yscB* mutants but not the *lcrG* mutant, which is required for LcrV secretion. Further, the contact sites between YscF and LcrV may be identified by the use of a suppressor screen for $yscF_{D28A,D46A}$ mutants, devised to restore the calcium-blind phenotype of strains also expressing wild-type *lcrV*. Lastly, the C-terminal end of LcrV may interact directly with YopD during the assemblies of the needle cap and injectisome. Of note, cap assembly does not require YopD (11); however, without YopD (or YopB), the cap cannot advance to generate an injectisome for effector translocation (19).

We noted phenotypic similarities but also differences for Strep-tagged LcrV mutants expressed in *Y. enterocolitica* or *Y. pestis*. $LcrV_{S270}$ and $LcrV_{S324}$ did not complement the Δ*lcrV* phenotype in *Y. enterocolitica* or in *Y. pestis*. Further, $LcrV_{S324}$ displayed a dominant negative LCR^- phenotype as well as a block in effector translocation in both *Y. enterocolitica* and *Y. pestis*. $LcrV_{S270}$ did not bind to LcrG, and the mutant protein was not a substrate for type III secretion. The $lcrV_{170}$ allele complemented the LCR^- phenotype of the *Y. pestis* Δ*lcrV* mutant and enabled type III secretion of YopE and $LcrV_{170}$. Nevertheless, $lcrV_{170}$ failed to restore effector translocation in both *Y. pestis* and *Y. enterocolitica* Δ*lcrV* mutants. Although $LcrV_{S170}$ did not bind to Strep-Tactin resin, the mutant copurified with GST-LcrG. Taken together, these data suggest that $LcrV_{S170}$, similarly to $LcrV_{S324}$, may assemble into a needle cap that is defective for injectisome assembly. In contrast, $LcrV_{S270}$ cannot bind LcrG and appears not to be secreted by *Yersinia*. These results are in agreement with earlier work identifying

TABLE 3 $LcrV_{S324}$ blocks type III secretion of YopH in *Y. pestis* calcium-blind mutants with $yscF_{D28A}$ and $yscF_{D46A}$ mutations

	Y. pestis (Δ*yopE*/*sycE*) % type III secretion ([S]/[S+P])[a]			
	No plasmid		p$lcrV_{S324}$	
yscF allele	YopH	LcrV	YopH	LcrV
yscF	45.2	42.7	2.9	5.3
$yscF_{D28A}$	44.9	39.8	4.5	18.2
$yscF_{D46A}$	45.8	29.1	4.4	15.3
$yscF_{D28A,D46A}$	47.3	45.8	2.2	9.3
$yscF_{D77A}$	0.9	1.1	3.3	4.9

[a] Type III secretion of *Y. pestis* strains with or without p$lcrV_{S324}$ was measured after 3 h of growth in cultures that were grown in media with chelated calcium ions at 37°C. Following centrifugation, the extracellular medium was separated into the supernatant (S) and the bacterial pellet (P), and proteins in both fractions were precipitated with trichloroacetic acid and analyzed by immunoblotting with specific antibodies against the type III secretion substrates YopH and LcrV. Secretion was quantified by calculating the percent amount of secreted protein [S] compared to protein in both the medium and the pellet [S+P].

residues 277, 289, and 292 as sites of 5-residue linker insertions that abolished the association between mutant LcrV and LcrG (47). Finally, $LcrV_{S20}$ and $LcrV_{S55}$ are secreted by Δ*lcrV* mutant *Y. pestis* and *Y. enterocolitica*. In *Y. enterocolitica*, $lcrV_{S20}$ and $lcrV_{S55}$ restore YopE secretion and effector translocation, whereas in *Y. pestis*, $lcrV_{S20}$ and $lcrV_{S55}$ cause a dominant negative LCR^- phenotype and a block in effector translocation. These data suggest that $LcrV_{S20}$ and $LcrV_{S55}$ form a functional needle cap in *Y. enterocolitica*. In contrast, $LcrV_{S20}$ and $LcrV_{S55}$ needle cap assembly may occur in *Y. pestis*; however, if formed, these caps cannot respond to the low-calcium signal or activate effector translocation. Of note, the alleles $lcrV_{S20}$ and $lcrV_{S55}$ enabled us to identify for the first time LcrV mutants that exert different phenotypes when expressed in *Y. enterocolitica* and *Y. pestis*. Thus, these mutants may be useful in elucidating the subtle differences between *Y. enterocolitica* and *Y. pestis* type III machines.

Sato and colleagues performed linker-scanning mutagenesis of *pcrV*, encoding the cap protein of *Pseudomonas aeruginosa* type III needles (48). Of note, PcrV and LcrV are 37% identical and 67% similar at the amino acid level, and the two proteins are presumed to assemble into structures with similar functions (43, 49). The insertion of a 19-residue linker at position 119 (D^{151}), 120 (S^{152}), 131 (L^{153}), 134 (E^{156}), 138 (L^{160}), or 279 (F^{308}) of PcrV abolished effector translocation in *P. aeruginosa* (in parentheses are the corresponding residues of the $LcrV_{W22703}$ orthologue) (48). The linker insertions map to helices α7 and α12 of LcrV, and the insertions likely interfere with the binding of mutant PcrV to PcrG, the LcrG orthologue in *P. aeruginosa* (48, 50).

ACKNOWLEDGMENTS

We thank members of our laboratory for critical comments and discussion. We also thank Antoni Hendrickx for guidance with transmission electron microscopy experiments.

This work was supported by a grant (AI42797) from the National Institute of Allergy and Infectious Diseases (NIAID), Infectious Diseases Branch (to O.S.). K.G.L. was a trainee of the Graduate Training in Growth and Development program at the University of Chicago (grant HD009007). The authors acknowledge membership within and support from the Region V "Great Lakes" Regional Center of Excellence in Biodefense and Emerging Infectious Diseases Consortium (NIH award 1-U54-AI-057153).

REFERENCES

1. **Cornelis GR, Boland A, Boyd AP, Geuijen C, Iriarte M, Neyt C, Sory MP, Stainier I.** 1998. The virulence plasmid of *Yersinia*, an antihost genome. Microbiol. Mol. Biol. Rev. **62**:1315–1352.
2. **Rosqvist R, Bolin I, Wolf-Watz H.** 1988. Inhibition of phagocytosis in *Yersinia pseudotuberculosis*: a virulence plasmid-encoded ability involved in the Yop2b protein. Infect. Immun. **56**:2139–2143.
3. **Perry RD, Harmon PA, Bowmer WS, Straley SC.** 1986. A low-Ca^{2+} response operon encodes the V antigen of *Yersinia pestis*. Infect. Immun. **54**:428–434.
4. **Cornelis GR.** 2002. *Yersinia* type III secretion: send in the effectors. J. Cell Biol. **158**:401–408.
5. **Rosqvist R, Magnusson KE, Wolf-Watz H.** 1994. Target cell contact triggers expression and polarized transfer of *Yersinia* YopE cytotoxin into mammalian cells. EMBO J. **13**:964–972.
6. **Cornelis GR.** 2006. The type III injectisome. Nat. Rev. Microbiol. **4**:811–825.
7. **Sorg JA, Blaylock B, Schneewind O.** 2006. Secretion signal recognition by YscN, the *Yersinia* type III secretion ATPase. Proc. Natl. Acad. Sci. U. S. A. **103**:16490–16495.
8. **Galan JE, Wolf-Watz H.** 2006. Protein delivery into eukaryotic cells by type III secretion machines. Nature **444**:567–573.
9. **Hoiczyk E, Blobel G.** 2001. Polymerization of a single protein of the pathogen *Yersinia enterocolitica* into needles punctures eukaryotic cells. Proc. Natl. Acad. Sci. U. S. A. **98**:4669–4674.
10. **Diepold A, Wiesand U, Amstutz M, Cornelis GR.** 2012. Assembly of the *Yersinia* injectisome: the missing pieces. Mol. Microbiol. **85**:878–892.
11. **Mueller CA, Broz P, Muller SA, Ringler P, Erne-Brand F, Sorg I, Kuhn M, Engel A, Cornelis GR.** 2005. The V-antigen of *Yersinia* forms a distinct structure at the tip of injectisome needles. Science **310**:674–676.
12. **Sorg JA, Miller NC, Schneewind O.** 2005. Substrate recognition of type III secretion machines: testing the RNA signal hypothesis. Cell. Microbiol. **7**:1217–1225.
13. **Mueller CA, Broz P, Cornelis GR.** 2008. The type III secretion system tip complex and translocon. Mol. Microbiol. **68**:1085–1095.
14. **Pollack C, Straley SC, Klempner MS.** 1986. Probing the phagolysosomal environment of human macrophages with a Ca^{2+}-responsive operon fusion in *Yersinia pestis*. Nature **322**:834–836.
15. **Lee VT, Mazmanian SK, Schneewind O.** 2001. A program of *Yersinia enterocolitica* type III secretion reactions is triggered by specific host signals. J. Bacteriol. **183**:4970–4978.
16. **Nilles ML, Fields KA, Straley SC.** 1998. The V antigen of *Yersinia pestis* regulates Yop vectorial targeting as well as Yop secretion through effects on YopB and LcrG. J. Bacteriol. **180**:3410–3420.
17. **Lee VT, Tam C, Schneewind O.** 2000. LcrV, a substrate for *Yersinia enterocolitica* type III secretion, is required for toxin targeting into the cytosol of HeLa cells. J. Biol. Chem. **275**:36869–36875.
18. **Hakansson S, Schesser K, Persson C, Galyov EE, Rosqvist R, Homble F, Wolf-Watz H.** 1996. The YopB protein of *Yersinia pseudotuberculosis* is essential for the translocation of Yop effector proteins across the target cell plasma membrane and displays a contact-dependent membrane disrupting activity. EMBO J. **15**:5812–5823.
19. **Hakansson S, Bergman T, Vanooteghem JC, Cornelis G, Wolf-Watz H.** 1993. YopB and YopD constitute a novel class of *Yersinia* Yop proteins. Infect. Immun. **61**:71–80.
20. **Goguen JD, Yother J, Straley SC.** 1984. Genetic analysis of the low calcium response in *Yersinia pestis* Mud1(Ap *lac*) insertion mutants. J. Bacteriol. **160**:842–848.
21. **Torruellas J, Jackson MW, Pennock JW, Plano GV.** 2005. The *Yersinia pestis* type III secretion needle plays a role in the regulation of Yop secretion. Mol. Microbiol. **57**:1719–1733.
22. **Yother J, Goguen JD.** 1985. Isolation and characterization of Ca^{2+}-blind mutants of *Yersinia pestis*. J. Bacteriol. **164**:704–711.
23. **Skrzypek E, Straley SC.** 1995. Differential effects of deletions in *lcrV* on secretion of V antigen, regulation of the low-Ca^{2+} response, and virulence of *Yersinia pestis*. J. Bacteriol. **177**:2530–2542.
24. **Skrzypek E, Straley SC.** 1993. LcrG, a secreted protein involved in negative regulation of the low-calcium response in *Yersinia pestis*. J. Bacteriol. **175**:3520–3528.
25. **Nilles ML, Williams AW, Skrzypek E, Straley SC.** 1997. *Yersinia pestis* LcrV forms a stable complex with LcrG and may have a secretion-related regulatory role in the low-Ca^{2+} response. J. Bacteriol. **179**:1307–1316.
26. **Burrows TW.** 1956. An antigen determining virulence in *Pasteurella pestis*. Nature **177**:426–427.
27. **DeBord KL, Anderson DM, Marketon MM, Overheim KA, DePaolo RW, Ciletti NA, Jabri B, Schneewind O.** 2006. Immunogenicity and protective immunity against bubonic plague and pneumonic plague by immunization of mice with the recombinant V10 antigen, a variant of LcrV. Infect. Immun. **74**:4910–4914.
28. **Derewenda U, Mateja A, Devedjiev Y, Routzahn KM, Evdokimov AG, Derewenda ZS, Waugh DS.** 2004. The structure of *Yersinia pestis* V-antigen, an essential virulence factor and mediator of immunity against plague. Structure **12**:301–306.
29. **Brubaker RR.** 1969. Mutation rate to non-pigmentation in *Pasteurella pestis*. J. Bacteriol. **98**:1404–1406.
30. **Higuchi K.** 1970. An improved chemically defined culture medium for strain L mouse cells based on growth responses to graded levels of nutrients including iron and zinc ions. J. Cell. Physiol. **75**:65–72.
31. **Cornelis GR, Colson C.** 1975. Restriction of DNA in *Yersinia enterocolitica* detected by the recipient ability for a derepressed R factor from *Escherichia coli*. J. Gen. Microbiol. **87**:285–291.
32. **Cheng LW, Anderson DM, Schneewind O.** 1997. Two independent type III secretion mechanisms for YopE in *Yersinia enterocolitica*. Mol. Microbiol. **24**:757–765.
33. **Miller NC, Quenee LE, Elli D, Ciletti N, Schneewind O.** 2012. Polymor-

phisms in the *lcrV* gene of *Yersinia enterocolitica* do not provide for escape from plague protective immunity. Infect. Immun. **80**:1572–1582.
34. **Ferracci F, Schubot FD, Waugh DS, Plano GV.** 2005. Selection and characterization of *Yersinia pestis* YopN mutants that constitutively block Yop secretion. Mol. Microbiol. **57**:970–987.
35. **Blaylock B, Berube BJ, Schneewind O.** 2010. YopR impacts type III needle polymerization in *Yersinia* species. Mol. Microbiol. **75**:221–229.
36. **Olsson J, Edqvist PJ, Bröms JE, Forsberg A, Wolf-Watz H, Francis MS.** 2004. The YopD translocator of *Yersinia pseudotuberculosis* is a multifunctional protein comprised of discrete domains. J. Bacteriol. **186**:4110–4123.
37. **Ramamurthi KS, Schneewind O.** 2002. Type III protein secretion in *Yersinia* species. Annu. Rev. Cell Dev. Biol. **18**:107–133.
38. **Cornelis G, Vanootegem JC, Sluiters C.** 1987. Transcription of the yop regulon from Y. enterocolitica requires trans acting pYV and chromosomal genes. Microb. Pathog. **2**:367–379.
39. **Michiels T, Wattiau P, Brasseur R, Ruysschaert JM, Cornelis G.** 1990. Secretion of Yop proteins by yersiniae. Infect. Immun. **58**:2840–2849.
40. **Anderson DM, Ramamurthi KS, Tam C, Schneewind O.** 2002. YopD and LcrH regulate the expression of *Yersinia enterocolitica* YopQ at a post-transcriptional step and bind to *yopQ* mRNA. J. Bacteriol. **184**:1287–1295.
41. **DeBord K, Lee VT, Schneewind O.** 2001. Roles of LcrG and LcrV during the type III targeting of effector Yops by *Yersinia enterocolitica.* J. Bacteriol. **183**:4588–4598.
42. **Quenee LE, Ciletti NA, Elli D, Hermanas T, Schneewind O.** 2011. Prevention of pneumonic plague in mice, rats, guinea pigs and non-human primates with clinical grade rV10, rV10-2 or F1-V vaccines. Vaccine **29**:6572–6583.
43. **Broz P, Mueller CA, Muller SA, Phillipsen A, Sorg I, Engel A, Cornelis GR.** 2007. Function and molecular architecture of the *Yersinia* injectisome tip complex. Mol. Microbiol. **65**:1311–1320.
44. **Quenee LE, Berube B, Segal J, Elli D, Ciletti NA, Anderson DM, Schneewind O.** 2010. Amino acid residues 196–225 of LcrV represent a plague protective epitope. Vaccine **28**:1870–1876.
45. **Benner GE, Andrews GP, Byrne WR, Strachan SD, Sample AK, Heath DG, Friedlander AM.** 1999. Immune response to *Yersinia* outer proteins and other *Yersinia pestis* antigens after experimental infection in mice. Infect. Immun. **67**:1922–1928.
46. **Ivanov MI, Noel BL, Rampersaud R, Mena P, Benach JL, Bliska JB.** 2008. Vaccination of mice with a Yop translocon complex elicits antibodies that are protective against infection with F1$^-$ *Yersinia pestis.* Infect. Immun. **76**:5181–5190.
47. **Hamad MA, Nilles ML.** 2007. Structure-function analysis of the C-terminal domain of LcrV from *Yersinia pestis.* J. Bacteriol. **189**:6734–6739.
48. **Sato H, Hunt ML, Weiner JJ, Hansen AT, Frank DW.** 2011. Modified needle-tip PcrV proteins reveal distinct phenotypes relevant to the control of type III secretion and intoxication by *Pseudomonas aeruginosa.* PLoS One **6**:e18356. doi:10.1371/journal.pone.0018356.
49. **Sato H, Frank DW.** 2011. Multi-functional characteristics of the *Pseudomonas aeruginosa* type III needle-tip protein, PcrV; comparison to orthologs in other Gram-negative bacteria. Front. Microbiol. **2**:142. doi:10.3389/fmicb.2011.00142.
50. **Lee PC, Stopford CM, Svenson AG, Rietsch A.** 2010. Control of effector export by the *Pseudomonas aeruginosa* type III secretion proteins PcrG and PcrV. Mol. Microbiol. **75**:924–941.